

AGILE observation of a gamma-ray flare from the blazar 3C 279

A. Giuliani¹, F. D’Ammando^{2,3}, S. Vercellone¹, V. Vittorini^{2,4}, A. W. Chen^{1,4}, I. Donnarumma², L. Pacciani², G. Pucella², A. Trois², A. Bulgarelli⁵, F. Longo⁶, M. Tavani^{2,3}, G. Tosti⁷, D. Impiombato⁷, A. Argan², G. Barbiellini⁶, F. Boffelli^{8,9}, P. A. Caraveo¹, P. W. Cattaneo⁸, V. Cocco², E. Costa², E. Del Monte², G. De Paris², G. Di Cocco⁵, Y. Evangelista², M. Feroci², M. Fiorini¹, F. Fornari¹, T. Froyland^{3,4}, F. Fuschino⁵, M. Galli¹⁰, F. Gianotti⁵, C. Labanti⁵, Y. Lapshov², F. Lazzarotto², P. Lipari¹¹, M. Marisaldi⁵, S. Mereghetti¹, A. Morselli¹², A. Pellizzoni¹, F. Perotti¹, P. Picozza¹², M. Prest¹³, M. Rapisarda¹⁴, A. Rappoldi⁸, P. Soffitta², M. Trifoglio⁵, E. Vallazza⁶, A. Zambra¹, D. Zanello⁹, S. Cutini¹⁵, D. Gasparri¹⁵, C. Pittori¹⁵, B. Preger¹⁵, P. Santolamazza¹⁵, F. Verrecchia¹⁵, P. Giommi¹⁵, S. Colafrancesco¹⁵, and L. Salotti¹⁶

¹ INAF/IASF–Milano, via E. Bassini 15, 20133 Milano, Italy
e-mail: giuliani@iasf-milano.inaf.it

² INAF/IASF–Roma, via Fosso del Cavaliere 100, 00133 Roma, Italy

³ Dip. di Fisica, Univ. “Tor Vergata”, via della Ricerca Scientifica 1, 00133 Roma, Italy

⁴ CIFS–Torino, Viale Settimio Severo 3, 10133 Torino, Italy

⁵ INAF/IASF–Bologna, via Gobetti 101, 40129 Bologna, Italy

⁶ Dip. di Fisica and INFN, via Valerio 2, 34127 Trieste, Italy

⁷ Dip. di Fisica, Univ. di Perugia, via Pascoli, 06123 Perugia, Italy

⁸ INFN–Pavia, via Bassi 6, 27100 Pavia, Italy

⁹ Dip. Fisica Nucleare e Teorica, Univ. di Pavia, via Bassi 6, 27100 Pavia, Italy

¹⁰ ENEA–Bologna, via dei Martiri di Monte Sole 4, 40129 Bologna, Italy

¹¹ INFN–Roma “La Sapienza”, Piazzale A. Moro 2, 00185 Roma, Italy

¹² INFN–Roma “Tor Vergata”, via della Ricerca Scientifica 1, 00133 Roma, Italy

¹³ Dip. di Fisica, Univ. dell’Insubria, via Valleggio 11, 22100 Como, Italy

¹⁴ ENEA–Roma, via E. Fermi 45, 00044 Frascati (Roma), Italy

¹⁵ ASI–ASDC, via G. Galilei, 00044 Frascati (Roma), Italy

¹⁶ ASI, Viale Liegi 26, 00198 Roma, Italy

Received 11 August 2008 / Accepted 10 October 2008

ABSTRACT

Context. We report the detection by the AGILE satellite of an intense gamma-ray flare from the gamma-ray source 3EG J1255-0549, associated with the Flat Spectrum Radio Quasar 3C 279, during the AGILE pointings towards the Virgo Region on 2007 July 9–13.

Aims. The simultaneous optical, X-ray and gamma-ray covering allows us to study the spectral energy distribution (SED) and the theoretical models relative to the mid-July flaring episode.

Methods. AGILE observed the source during its Science Performance Verification Phase with its two co-aligned imagers: the Gamma-Ray Imaging Detector (GRID) and the hard X-ray imager (Super-AGILE) sensitive in the 30 MeV–50 GeV and 18–60 keV respectively. During the AGILE observation the source was monitored simultaneously in the optical band by the REM telescope and in the X-ray band by the *Swift* satellite through 4 target of opportunity observations.

Results. During 2007 July 9–13, AGILE-GRID detected gamma-ray emission from 3C 279, with the source at $\sim 2^\circ$ from the center of the field of view, with an average flux of $(210 \pm 38) \times 10^{-8}$ ph cm⁻² s⁻¹ for energy above 100 MeV. No emission was detected by Super-AGILE, with a $3\text{-}\sigma$ upper limit of 10 mCrab. During the observation, which lasted about 4 days, no significant gamma-ray flux variation was observed.

Conclusions. The Spectral Energy Distribution is modelled with a homogeneous one-zone Synchrotron Self Compton emission plus the contributions by external Compton scattering of the direct disk radiation and, to a lesser extent, by external Compton scattering of photons from the Broad Line Region.

Key words. gamma rays: observations – galaxies: quasars: individual: 3C 279

1. Introduction

3C 279 ($z = 0.536$) is an optically violent variable (OVV) quasar, the first and one of the brightest blazars discovered in the gamma-ray band by EGRET (Hartman et al. 1992).

Despite its relatively large distance this FSRQ is probably the most intensively studied blazar in every band of the

electromagnetic spectrum. Its SED has two broad bumps with the first peak occurring at the far-IR ($\sim 10^{13}$ Hz) and the second one extending in the MeV-GeV energy range. 3C 279 is highly variable at all frequencies of the spectrum, particularly in the high frequency part of the two bumps, showing a variability on time scales ranging from days to months. This behavior is usually interpreted assuming that the first peak is due to the

synchrotron emission of highly relativistic electrons accelerated in a jet stemming from the nucleus, and the second peak generated by the Inverse Compton (IC) emission of the same electrons interacting with low-energy photons produced by the jet itself (Synchrotron Self Compton, SSC) or by a region external to the jet (External Compton, EC).

3C 279 is the first quasar that exhibited apparent superluminal motion (Whitney et al. 1989) and high-resolution VLBI radio maps show correlations between flare activity and components ejected from the core (Wehrle et al. 2001). The observation of radio blobs emitted by 3C 279 (Lindfords et al. 2006) strongly supports the presence of a jet. It has been argued that the misalignment between the jet and the line of sight is only two degrees (Lindfords et al. 2005).

3C 279 has been detected several times in the gamma-rays energy band by the EGRET instrument on board *CGRO* (Hartman et al. 2001) with integrated flux changes of up to a factor of 100.

The gamma-ray emission exhibited the largest amplitude variability on both long (months) and short (days) time scales. On the basis of historical gamma-ray observations it is possible to distinguish between high states (average flux equal to or greater than about 10^{-6} ph cm $^{-2}$ s $^{-1}$ above 100 MeV) and low states (average flux of the order of 10^{-7} ph cm $^{-2}$ s $^{-1}$). The photon indices of the gamma-ray energy spectra during the different levels of activity of the source range from 1.7 to 2.4; a correlation between average fluxes and spectral indices is still debated (Nandikotkur et al. 2007; Hartman et al. 2001).

3C 279 was also detected by OSSE (50 keV–1 MeV) at the transition region from hard X-rays and gamma-rays and COMPTEL at low energy (1–30 MeV) gamma-rays (McNaron-Brown et al. 1995). Although flux variations were found in the OSSE and EGRET energy bands, only marginal flux variations were observed in the COMPTEL energy band. Hartman et al. (2001) argued that this behaviour could be explained by considering the Comptonization of direct accretion disc photons at COMPTEL energies and the Comptonization of accretion disc photons scattered in the jet region by the Broad Line Region (BLR) clouds at EGRET energies.

Evidence for a thermal component due to the emission from the accretion disk was noted by Pian et al. (1999). This Seyfert-like component, present in other blazar such as 3C 454.3 (Raiteri et al. 2007) and AO 0235+164 (Raiteri et al. 2006), is detected only in low activity states of the sources, when the contribution of the beamed synchrotron radiation is less important. This could explain the smaller variability observed in the UV than in the optical band, under the assumption that the disk emission is not variable on time scales of less than a few years. Instead, in the optical band 3C 279 varies dramatically on different time scales ranging from intense outbursts that last about one year to microvariability on the scale of hours (see e.g. Kartaltepe & Balonek 2007). Historically the source has a R-band magnitude ranging between 12.5 and 16.5. The variability profile of the observed flares seems to be consistent with the optical emission of 3C 279 being dominated by synchrotron emission produced in the strong magnetic field of the relativistic jet.

Recently the MAGIC telescope has detected very high energy (VHE) gamma-rays from 3C 279 (Albert et al. 2008). The detection of the VHE gamma-ray emission from a source at such a distance could constrain the current theories about the density of the extragalactic background light (EBL), providing an indication that the Universe appears more transparent at cosmological distance than believed.

In this letter we present the analysis of the AGILE observation of 3C 279 between 9 July 2007 and 13 July 2007.

2. AGILE data

2.1. AGILE observation of 3C 279

AGILE (Astrorivelatore Gamma a Immagini LEggero) is an Italian Space Agency (ASI) mission (Tavani et al. 2008) devoted to high-energy astrophysics studies.

The satellite was successfully launched from the Indian base of Sriharikota on 23 April 2007 and has the peculiar characteristic of operating simultaneously in the hard X-ray and gamma-ray energy bands yielding broad-band coverage in the energy spectrum. The AGILE instrument combines the Gamma Ray Imaging Detector (GRID) sensitive in the energy range 30 MeV–50 GeV and the X-ray coded-mask imager SuperAGILE (Feroci et al. 2007) sensitive in the energy range 18–60 keV. The GRID instrument is composed of a pair-production tracker based on silicon microstrip technology (Silicon Tracker; Prest et al. 2003; Barbiellini et al. 2001), a calorimeter made of CsI bars (Mini-Calorimeter; Labanti et al. 2006) placed below the Silicon Tracker and an anti-coincidence system (ACS) segmented in 13 panels of plastic scintillators (Perotti et al. 2006).

The Silicon Tracker and the on-board trigger logic are optimized for gamma-ray imaging in the 30 MeV–50 GeV energy band (Argan et al. 2004).

At the beginning of the Science Performance Verification Phase, AGILE repointed to the Virgo region and observed the blazar 3C 279 for a total of 44 h of effective time. The source was close (about 2 degrees) to the center of the field of view of the instrument for the whole observing time. Super-AGILE observed 3C 279 for a total on-source net exposure time of about 100 ks.

2.2. Data reduction and analysis

Level-1 AGILE-GRID data were analyzed using the AGILE Standard Analysis Pipeline. The ACS and a set of hardware triggers perform the first reduction of the high rate of background events (charged particles and albedo gamma-rays) interacting with the instrument. A dedicated software processes the signals coming from the GRID and the ACS, performing a reconstruction and selection of events in order to discriminate between background events and gamma-rays, deriving for the latter the energy and direction of the incoming photons. A simplified version of this software operates directly on board AGILE in order to reduce the telemetry throughput (Giuliani et al. 2006). A more complex version of the reconstruction and selection software is applied on the ground, producing a photon list containing the arrival time, energy and direction of each gamma-ray and the corresponding exposure maps.

Counts, exposure and Galactic background gamma-ray maps, the latter based on the diffuse emission model developed for AGILE (Giuliani et al. 2004), were created with a bin-size of 0.25×0.25 for photons with an energy greater than 100 MeV. We selected only events flagged as confirmed gamma-ray events, and all events collected during the South Atlantic Anomaly and whose reconstructed directions form angles with the satellite-Earth vector of less than 80° are rejected.

In order to derive the average flux and spectrum of the source we run the AGILE maximum likelihood procedure (Chen et al. 2008) on the whole observing period, according to Mattox et al. (1993).

3. Optical and X-ray observations

3.1. Swift observation

The Swift X-ray Telescope (XRT; Burrows et al. 2004, 0.2–10 keV) data were processed with standard procedures (xrtpipeline v0.11.6) adopting the standard filtering and screening criteria. All the observations were performed in photon counting (PC) mode and photons were selected with grades in the range 0–12.

Swift-XRT uncertainties are given at a 90% confidence level for one interesting parameter unless otherwise stated. Data were rebinned in order to have at least 20 counts per energy bin and to use the χ^2 statistics.

Spectral analysis was performed using the Xspec fitting package 12.3.1, with the results shown in Table 1. We fit the spectra with an absorbed power law with Galactic absorption fixed at $N_{\text{H}} = 2.05 \times 10^{20} \text{ cm}^{-2}$ (wabs*powerlaw model in Xspec).

3.2. REM observation

The photometric optical observations were carried out with the Rapid Eye Mount (REM, Zerbi et al. 2004), a robotic telescope located at the ESO Cerro La Silla observatory (Chile). The REM telescope has a Ritchey-Chretien configuration with a 60 cm f/2.2 primary and an overall f/8 focal ratio in a fast moving alt-azimuth mount providing two stable Nasmyth focal stations. At one of the two foci the telescope simultaneously feeds, by means of a dichroic filter, two cameras: REMIR for the NIR (Conconi et al. 2004) and ROSS for the optical (Tosti et al. 2004), used in order to obtain nearly simultaneous data. For a detailed description of the data reduction and analysis see e.g. Dolcini et al. (2007).

The telescope REM has continuously observed 3C 279 for about 1 year between December 2006 and December 2007, including the AGILE observation period. The light curve produced by REM in the R-band is shown in Fig. 3.

4. Results and discussion

During the period between 9 and 13 July 2007, AGILE detected a gamma-ray source with a position compatible with 3C 279 at a significance level of 11.1σ (see Fig. 1) with an average flux of $(210 \pm 38) \times 10^{-8} \text{ ph cm}^{-2} \text{ s}^{-1}$ for $E > 100 \text{ MeV}$, as derived from a maximum likelihood analysis using the radio position of the source ($l = 305.10^\circ$ $b = 57.06^\circ$). AGILE detected the source at a flux level comparable to that measured by EGRET when the source was in a flaring state. Fitting the gamma-ray fluxes with a constant model (the weighted mean of the 1-day average flux values) and following McLaughlin et al. (1996) we obtain a variability coefficient of $V = 0.32$, indicating that the source is not variable in gamma-ray band during the AGILE observation.

Figure 2 reports the average gamma-ray spectrum of 3C 279 for the AGILE observing period. Fitting the data with a simple power law model we obtain a photon index of $\Gamma = 2.22 \pm 0.23$. The photon index is calculated with the weighted least squares method, considering only three energy bins for the fit: 100–200 MeV, 200–400 MeV and 400–1000 MeV. The source was not detected (above 5σ) by the Super-AGILE Iterative Removal of Sources (IROS) applied to the image, in the 20–60 keV energy range. A 3σ upper limit of 10 mCrab was obtained from the observed count rate by a study of the background fluctuations at the position of the source and a simulation of the

Table 1. Results of XRT observations of 3C 279. Power law model with N_{H} fixed to the Galactic value of $2.05 \times 10^{20} \text{ cm}^{-2}$.

Observation date	Flux 2–10 keV $\text{erg cm}^{-2} \text{ s}^{-1}$	Spectral slope Γ	χ_r^2 (d.o.f.)
10-Jul.-2007	1.20×10^{-11}	1.42 ± 0.05	1.21 (73)
11-Jul.-2007	1.17×10^{-11}	1.47 ± 0.07	0.86 (52)
12-Jul.-2007	1.05×10^{-11}	1.47 ± 0.06	1.07 (57)
13-Jul.-2007	1.13×10^{-11}	1.48 ± 0.06	0.96 (50)

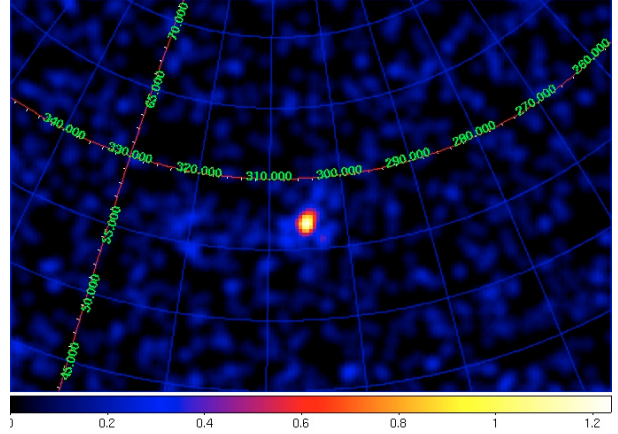


Fig. 1. Gaussian-smoothed counts map in Galactic coordinates for the 3C 279 region over the observing period 9–13 July 2007. Only photons with an energy greater than 100 MeV have been folded.

source and background contributions with IROS. Instead, Swift-XRT detected the source with daily observations between 10 and 13 July at a nearly constant flux of about $10^{-11} \text{ erg cm}^{-2} \text{ s}^{-1}$ (see Table 1).

The multiwavelength studies performed in the past on 3C 279 showed that during gamma ray flares most of the power emitted by the source lies in the high-energy gamma-ray band. In accordance with leptonic models for blazars, the high-energy peak in the blazars SED is due to inverse Compton emission from the relativistic electrons accelerated by the jet. In the case of 3C 279, the external Compton scattering of direct disk radiation (EDC) and external Compton scattering of radiation from cloud (ECC) components dominate in high-energy gamma-rays, yielding a total spectrum which varies as a function of the relative contribution of these two components.

A possible correlation between gamma-ray flux value and spectral index is the subject of debate (Nandikotkur et al. 2007), but EGRET observations of 3C 279 hinted at a gradual hardening during the flaring states that can be interpreted as the ECC component dominating during the flaring states. Only one flare (during EGRET observation P9) showed a soft spectrum that was EDC dominated. Our AGILE observation seems to be similar to the P9 flare, supporting the idea that a soft spectrum during flaring episodes is not an extremely rare event. Hartman et al. (2001) suggests that softening spectra can be due to a low state of the accretion disk that occurred before of the EGRET observation P9, which led to a reduction of the ECC component.

From the R-band light curve (Fig. 3) it emerges that a strong minimum occurred about 2 months before the period covered by the GRID observations (indicated by the yellow shaded region in the figure). This optical minimum might be correlated with a low accretion state of the disk; even if the relation between highly relativistic jets and accretion processes in AGN is one of the fundamental remaining problems in astrophysics, the

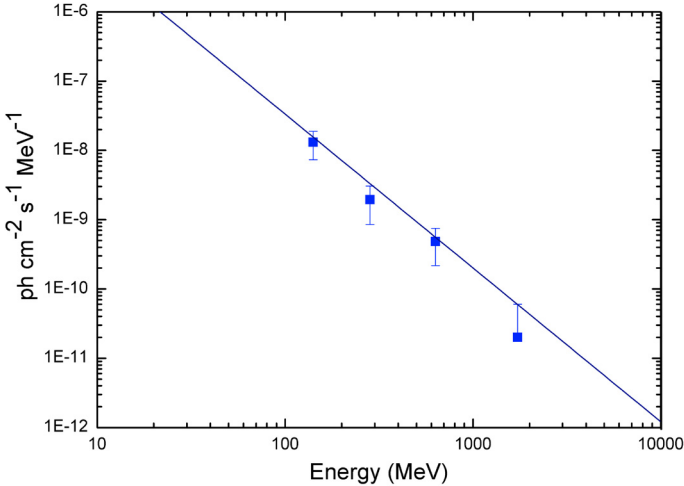


Fig. 2. Gamma-ray photon spectrum for 3C 279 during the observation period 9–13 July 2007. Four energy bins were taken into account: 100–200 MeV, 200–400 MeV, 400–1000 MeV, 1000–3000 MeV. The solid line corresponds to a power law function with photon index 2.22 ± 0.23 .

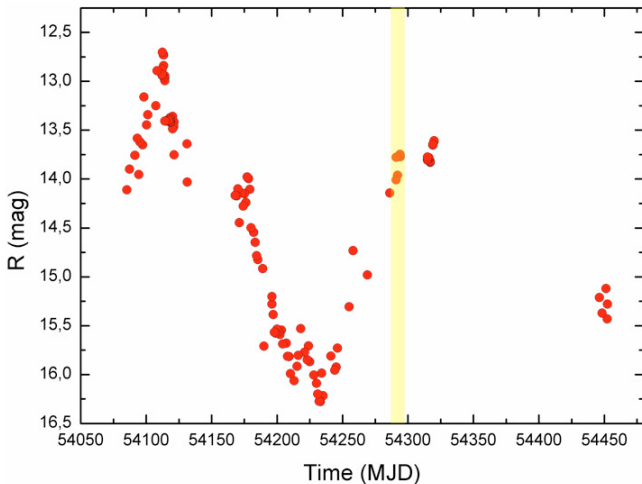


Fig. 3. Long-term R-band light curve as observed by REM between December 2006 and December 2007. The yellow shaded region indicates the period covered by the GRID observation.

current theoretical models of the formation of jet suggest that the power is generated by means of accretion, extracted from the disk rotational energy and converted into kinetic power of the jet (Blandford & Payne 1982). If the accretion rate is related to the jet power (see e.g. Ghisellini & Tavecchio 2008) then it is also related to the synchrotron emission seen in the optical band. In this scenario, the reduction of activity of the disk causes a decrease of the photon seed population produced by the disk and then an ECC component deficit; this effect was delayed by two months (roughly the light travel time from the inner disk to the broad line region) coincident with the AGILE observation period. To test this hypothesis we fit the optical, X-ray and gamma-ray data with an SCC+EC model similar to the model used to fit the P9 EGRET observation in Hartman et al. (2001) but with different parameter values, finding a good agreement with the data. We use a double power law distribution for the electron's energy density with spectral index $p_1 = 2.0$ from $\gamma_{\min} = 100$ to $\gamma_{\text{break}} = 600$ and $p_2 = 4.0$ for γ over 600, with a density at break $n_e = 30 \text{ cm}^{-3}$ and $\gamma_{\max} = 6 \times 10^3$.

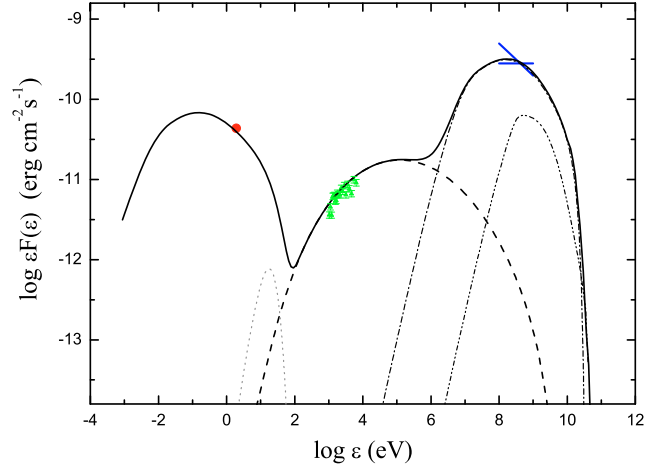


Fig. 4. Spectral energy distribution of 3C 279 for the AGILE-GRID observation, including simultaneous optical (REM) and X-ray (Swift) data. The dotted, dashed, dot-dashed and double-dot dashed lines represent the contributions of the accretion disk blackbody, the SSC, the external Compton scattering of disk radiation and the external Compton scattering of radiation from clouds, respectively.

The blob has a radius $R = 2.5 \times 10^{16} \text{ cm}$, magnetic field $B = 1.8 \text{ Gauss}$ and it moves with a bulk Lorentz factor $\Gamma = 13$ at an angle $\theta = 2^\circ$ with respect to the line of sight. The relativistic Doppler factor is then $\delta = 21.5$. The accretion disk luminosity assumed is $L_d = 5 \times 10^{45} \text{ erg s}^{-1}$ with a broad line region reprocessing 10% of the illuminating continuum. Figure 4 shows the SED for the GRID observing period, including simultaneous optical (REM) and X-ray (Swift) data and indicating individual model components.

5. Conclusions

During the period 2007 June 9–13 AGILE detected a highly significant source (11.1 sigma for $E > 100 \text{ MeV}$) associated with the FSRQ 3C 279. The source had an average flux of $(210 \pm 38) \times 10^{-8} \text{ ph cm}^{-2} \text{ s}^{-1}$ over the period covered by the AGILE observation. Gamma-ray flux variations on a 1-day time scale seem not to be present in our data, while longer timescales cannot be investigated due to the short observing time. The spectra measured by AGILE are compatible with a power law distribution of slope 2.22 ± 0.23 in the energy range 100 MeV–1 GeV. This soft spectrum observed during a flaring episode, already observed during the EGRET P9 observation, could be an indication of a dominant contribution of the EDC emission compared to ECC emission. The Inverse Compton scattering of relativistic electrons of synchrotron or ambient photons is responsible for the emission at hard X-ray and gamma-ray energies for FSRQ as 3C 279. Clarifying the exact nature of the seed photons for the IC scattering would explain the origin of the huge amplitude variations exhibited by 3C 279 at the highest energies.

Acknowledgements. The AGILE Mission is funded by the Italian Space Agency (ASI) with scientific and programmatic participation by the Italian Institute of Astrophysics (INAF) and the Italian Institute of Nuclear Physics (INFN). We wish to express our gratitude to the Carlo Gavazzi Space, Thales Alenia Space, Telespazio and ASDC/Dataspaio Teams that implemented the necessary procedures to carry out the AGILE re-pointing. *Facilities:* AGILE

References

- Albert, J., Aliu, E., Anderhub, H., et al. 2008, *Science*, 320, 1752
- Argan, A., et al. 2004, *Proceedings IEEE-NSS*, 1, 371
- Barbiellini, G., Bordignon, G., Fedel, G., et al. 2001, in *Gamma 2001: Gamma-Ray Astrophysics*, ed. S. Ritz, N. Gehrels, & C. R. Shrader, AIP Conf. Ser., 587, 754
- Blandford, R. D., & Payne, D. G. 1982, *MNRAS*, 199, 883
- Burrows, D. N., Hill, J. E., Nousek, J. A., et al. 2005, *Space Sci. Rev.*, 120, 165
- Chen, A., et al. 2008, in preparation
- Conconi, P., Cunniffe, R., D'Alessio, F., et al. 2004, *SPIE*, 5492, 1602
- Dolcini, A., Farfanelli, F., Ciprini, S., et al. 2007, *A&A*, 469, 503
- Feroci, M., Costa, E., Soffitta, P., et al. 2007, *NIM A*, 581, 728
- Ghisellini, G., & Tavecchio, F. 2008, *MNRAS*, 387, 1669
- Giuliani, A., Chen, A., Mereghetti, S., et al. 2004, *Mem. SAI Suppl.*, 5, 135
- Giuliani, A., Cocco, V., Mereghetti, S., et al. 2006, *NIM A*, 568, 692
- Hartman, R. C., Bertsch, D. L., Fichtel, C. E., et al. 1992, *ApJ*, 385, 1
- Hartman, R. C., Bertsch, D. L., Bloom, S. D., et al. 1999, *ApJS*, 123, 79
- Hartman, R. C., Böttcher, M., Aldering, G., et al. 2001, *ApJ*, 553, 683
- Kartaltepe, J. S., & Balonek, T. J. 2007, *AJ*, 133, 2866
- Labanti, C., Marisaldi, M., Fuschino, F., et al. 2006, in *Proc. SPIE*, 6266, 62663Q
- Lindfors, E. J., Valtoja, E., & Türler, M. 2005, *A&A*, 440, 845
- Lindfors, E. J., Türler, M., & Valtoja, E. 2006, *A&A*, 456, 895
- Mattox, J. R., Bertsch, D. L., Chiang, J., et al. 1993, *ApJ*, 410, 609
- McLaughlin, M. A., Mattox, J. R., Cordes, J. M., et al. 1996, *ApJ*, 473, 763
- McNaron-Brown, K., Johnson, W. N., Jung, G. V., et al. 1995, *ApJ*, 451, 575
- Nandikotkur, J., Jahoda, K. M., Hartman, R. C., et al. 2007, *ApJ*, 657, 706
- Perotti, F., Fiorini, M., Incorvaia, S., Mattaini, E., & Sant'Ambrogio, E. 2006, *NIM A*, 556, 228
- Pian, E., Urry, C. M., Maraschi, L., et al. 1999, *ApJ*, 521, 112
- Prest, M., Barbiellini, G., Bordignon, G., et al. 2003, *NIM A*, 501, 280
- Raiteri, C. M., Villata, M., Kadler, M. A., et al. 2006, *A&A*, 459, 731
- Raiteri, C. M., Villata, M., Larionov, V. M., et al. 2007, *A&A*, 473, 819
- Tavani, M., Barbiellini, G., Argan, A., et al. 2008, *A&A*, in press [arXiv:0807.4254]
- Tosti, G., Bagaglia, M., Campeggi, C., et al. 2004, *SPIE*, 5492, 689
- Unwin, S. C., Biretta, J. A., Hodges, M. W., et al. 1989, *ApJ*, 340, 117
- Wehrle, A. E., Piner, B. G., Unwin S. C., et al. 2001, *ApJS*, 133, 297
- Whitney, A. R., Shapiro, I. I., Rogers, A. E. E., et al. 1971, *Science*, 173, 225
- Zerbi, F. M., Chincarini, G., Ghisellini, G., et al. 2004, *SPIE*, 5492, 1590